CRYOLAVA DOME-FORMING ERUPTIONS ON EUROPA AND INFERENCES FOR THE EVOLUTION OF CRUSTAL FLUID RESERVOIRS. Lynnae C. Quick[1], Sarah A. Fagents[2], Ross A. Beyer[3,4], Chloe B. Beddingfield[3,4], Karla A. Nuñez[5], Louise M. Prockter[6], [1]NASA Goddard Space Flight Center, Greenbelt, MD 20771, Lynnae.C.Quick@nasa.gov, [2]The University of Hawai'i at Manoa, Honolulu, HI 96822, [3]The SETI Institute, Mountain View, CA 94043, [4]NASA Ames Research Center, Mountain View, CA 94035, [5]University of Maryland College Park, College Park, MD 20742, [6]Lunar and Planetary Institute, Houston TX 77058.

Introduction: We previously modeled a subset of domes on Europa with morphologies consistent with emplacement by viscous cryolava (Fig. 1) [1]. However, that approach only allowed for the investigation of late-stage eruptive processes far from the vent, and provided little insight into how cryolavas arrived at the surface. Consideration of dome emplacement as cryolavas erupt onto the surface, and the conditions in subsurface fluid reservoirs that would facilitate these eruptions, is therefore pertinent. A volume flux approach, in which lava erupts from the vent at a constant rate, was successfully applied to the formation of steep-sided volcanic domes on Venus [2]. These domes are believed to have formed in the same manner as candidate cryolava domes on Europa [1,3]. In order to better gauge the potential for dome formation on Europa via effusive eruptive events, we have applied this new approach to the formation of putative cryolava domes on Europa. Here we present the results of this modeling and explore conditions in subsurface fluid reservoirs that would enable dome-forming lava to be driven to the surface.

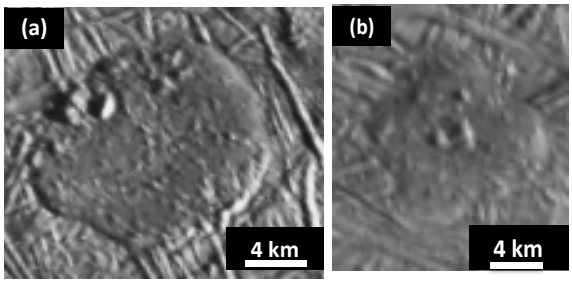

Figure 1. Candidate cryolava domes. (a) DEMs reveal that this dome has a central depression, suggesting that after emplacement, fluids were drawn back down into the subsurface. (b) The petal-shaped outline of this dome is consistent with the formation of flow lobes.

Approach: Assuming as in [1] that europan cryolavas are briny, aqueous solutions which may contain some ice crystal fraction, an alternative method for inferring bulk cryolava rheology, which incorporates the fluid emplacement stage, is presented here. An innovative perturbation solution to the generalized form of the Boussinesq equation for fluid flow in a cylindrical geometry is presented in [4]. The continuity equation describing radial expansion of a Newtonian fluid with an unbounded (free) upper surface is:

$$\frac{\partial h}{\partial t} - \frac{g}{3\nu}\frac{1}{r}\frac{\partial}{\partial r}\left(rh^3\frac{\partial h}{\partial r}\right) = 0 \qquad (1)$$

[4] found a similarity solution to (1) by transforming this equation to an ordinary differential equation when a constant volumetric flowrate, Q, at the origin is given. This similarity solution is found by perturbation by defining a parameter $\varepsilon = 1/(n+1)$ [2,4]. The new independent variable, x, and dependent variable P, that transform (1) to an ordinary differential equation are defined as:

$$x = \left(\frac{r^2}{4t}\right)\left[\varepsilon\Phi\left(\frac{Q}{4\pi\epsilon}\right)^{1-\varepsilon}\right]^{-1} \text{ and} \qquad (2)$$
$$P(x;\varepsilon) = 4\pi\varepsilon h^4/Q$$

where ε = ¼ and Φ = 1.2 for Europan cryolavas when a Newtonian rheology is assumed [2-4]. Following the approach from [4], flow thickness, h, as a function of time is described by:

$$h = h_o\left(P\frac{Q}{4\pi\varepsilon}\right)^{\varepsilon} \qquad (3)$$

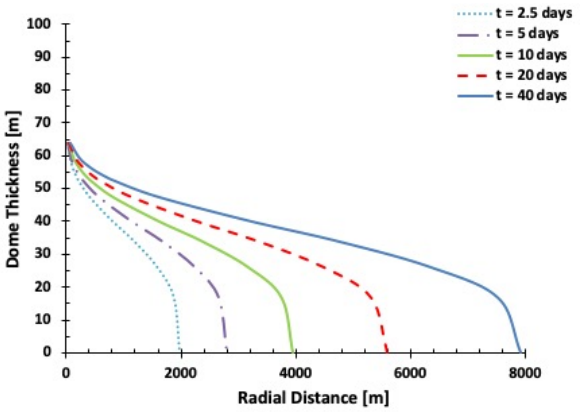

Figure 2. Axially symmetric Newtonian fluid flow profiles at five times when Q = 2000 m³/s at the vent.

Results: Fig. 2 shows the solution of a radially spreading, Newtonian fluid with a bulk kinematic viscosity, $\nu = 10^3$ m²/s (equivalent to a bulk dynamic viscosity, $\mu = 10^6$ Pa s). Here, the overall "shape" of the flow surface and the aspect ratio at t = 40 days is very similar to the dimensions of the dome in Fig. 1a. Note that the bulk kinematic viscosity reported above includes the contribution from the brittle cryolava crust [1, 5-6]. The initial viscosity of the erupted cryolava may be up to 4 orders of magnitude lower than this value [1, 5-7], perhaps as low as 10^{-1} m²/s. In a next iteration of this work, we will explore the effects on dome formation while varying ν and Q at the vent. We will also place bounds on plausible cryolava compositions that

are commensurate with the viscosity values obtained.

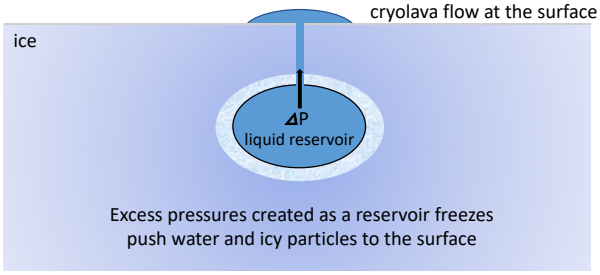

Figure 3. Cryolava domes may form when excess pressures created by the gradual freezing of crustal fluid reservoirs push viscous fluid to Europa's surface. Figure after [3].

Crustal Fluid Reservoirs: Excess pressures caused by the gradual freezing of crustal reservoirs will lead to stress conditions that promote fracturing in Europa's ice shell and that cause fluids to be driven to Europa's surface in these fractures (Fig. 3) [3, 8]. Thus, exploring the thermal evolution of fluid reservoirs in Europa's crust allows reasonable estimates to be placed on both the longevity of cryovolcanic eruptions at the surface, and the total volume of fluid that can be driven to the surface during each eruptive event [9]. The temperature, T, as a function of time, t, for spherical fluid reservoirs, embedded in Europa's ice shell may be expressed as:

$$T = T_{ice} + (T_o - T_{ice})\left(1 - e^{-r^2/4\kappa_{ice}t}\right) \quad (4)$$

[10] where T_{ice} is the local temperature of the ice shell surrounding the reservoir, T_o = 273 K and r are the reservoir's initial temperature and radius, respectively, and κ_{ice} is the thermal diffusivity of the surrounding ice. The total cooling time of the reservoir may be approximated as: $t_{total} = r^2/\kappa_{fluid}$ [11] where $\kappa_{fluid} = 10^{-7}$ m^2/s [3]. The reservoir is 100% crystallized at a time t_{total}. If it is then assumed that only a fraction of the reservoir is crystallized at all other times, t, a general relationship between % crystallinity and t is [11]:

$$\%_{reservoir\ crystallized} = \frac{t}{t_{total}} \times 100\ \% \quad (5)$$

Fig. 4 shows temperature as a function of time for a reservoir with r = 2 km located 1 km benath Europa's surface, assuming T_{ice} = 110 K and $\kappa_{ice} \cong 6 \times 10^{-6}$ m^2/s in (4). It is clear from Fig. 4 that $T \geq 200$ K for 6.5 x 10^3 years. Fig. 5 shows that at 10^4 years, the reservoir reaches ~ 60% crystallinity. At this time, the fluid within will be too viscous to be pushed to the surface and erupt [1,13]. Figs. 4 and 5 may be used to place bounds on the total eruption time of dome-forming cryolavas on Europa's surface. They show that cryolava issuing from a spherical reservoir that is 2 km in radius would be driven to the surface for a minimum of 6.5 x 10^3 years and a maximum of 10^4 years. In a next iteration of this model, we will couple our analyses to those of [3] and [9] to place constraints on the amount of time between reservoir emplacement in Europa's crust and cryovolcanic eruptions at the surface. We will also quantify the volume of fluid that is driven to the surface, as the reserovir cools, in order to constrain the eruption durations required to deliver the 10^9 m^3 of fluid to Europa's surface that represents the typical volume of europan cryolava domes [3, 13].

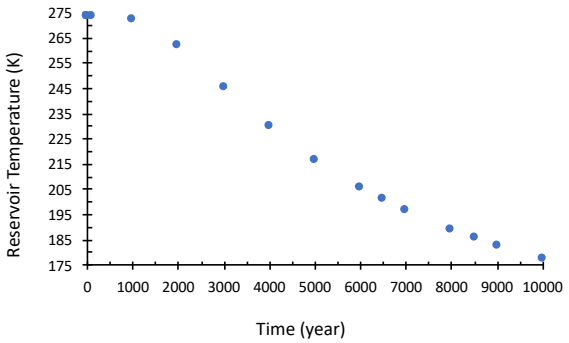

Figure 4. Temperature as a function of time for a spherical reservoir when r = 2 km. T = 273 K for the first 100 years and T ≥ 200 K for 6.5 x 10^3 years.

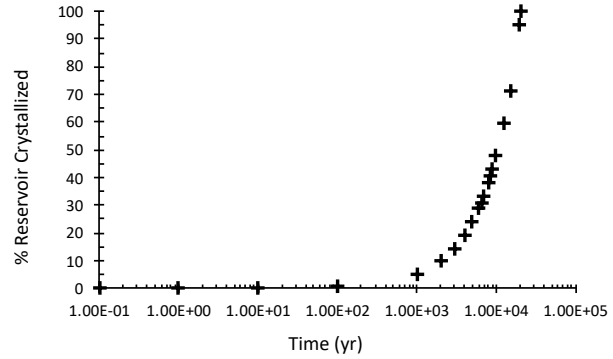

Figure 5. Gradual freezing of the reservoir as a function of time. After 10^4 years, 60% of the reservoir is frozen and the fluid within is too viscous to erupt onto Europa's surface.

References: [1] Quick, L. C. et al. (2017) *Icarus*, *284*, 477-488. [2] Quick, L. C. et al. (2016) *JVGR 319*, 93-105. [3] Fagents, S. A. (2003) *JGR, 32,* E12. [4] D. K. Babu & Van Genuchten, M. T. (1980) *J. Hydrol., 48*, 269-280. [5] Schenk, P. M. (1991) *JGR, 96,* 1887-1906. [6] Lorenz, R. D. (1996) *P&SS, 9*, 1021-1028. [7] Stofan, E. R. et al. (2000) *JGR,105*, 26,757-26,771. [8] Manga, M., Wang. C-Y. (2007) *GRL, 34*, L07202. [9] Lesage, E., et al. (2020) *Icarus, 335,* 113369. [10] Crank, J. (1975) *The Mathematics of Diffusion, Chapter 3,* pp. 28-30. [11] Quick, L. C. et al. (2019) *Icarus, 320*, 119-135. [12] Marsh, B. D. (1981) *Contrib. Mineral Petrol., 78*, 85-98. [13] Nuñez, K.A., et al. (2019) *50th LPSC*, Abstract #3264.